A Unifying Formulation for Discontinuous High-Order Methods

Z.J. Wang, H. Gao and T. Haga
Department of Aerospace Engineering and Computational Fluid Dynamics Center
Iowa State University, Ames, IA 50011

Presented at
7th Nobeyama Workshop on CFD:
To the Memory of Professor Kuwahara
University of Tokyo, Tokyo
September 23-24 2009

Outline

- Introduction
- Review of the Godunov finite volume and flux reconstruction formulation
- A unifying formulation on mixed meshes
  - Lifting collocation penalty approach
  - Connection with the DG, SV and SD method,
  - Extension to mixed meshes and curved boundaries;
- Sample numerical results
- Conclusions and future work

Motivation

- Most production/commercial codes only 1st or 2nd order accurate, i.e. $Error \propto h^p$ with p = 1 or 2
- Though adequate for a wide range of applications, many problems require higher-order accuracy. For example:
  - Aeroacoustic problems;
  - Vortex dominated flow …

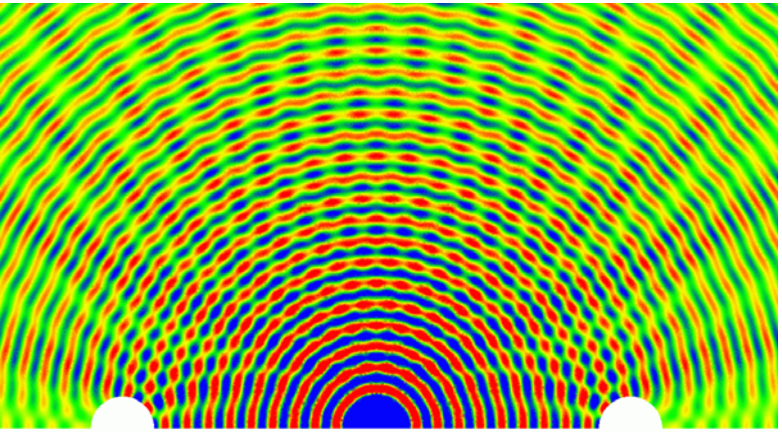

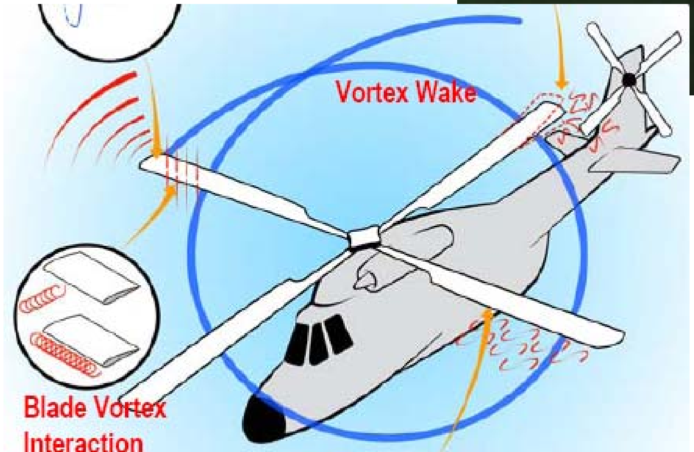

Introduction

- Many criteria can be used to classify high-order methods
  - Based on type of grids: structured grid vs. unstructured grid high-order methods
  - Based of the type of solutions: continuous or discontinuous high-order methods
- Continuous high-order methods
  - SUPG, RD, spectral element, …
- Discontinuous high-order methods:
  - Discontinuous Galerkin, staggered-grid, spectral volume, spectral difference, flux reconstruction, …

Review of Godunov FV Method

Consider

$$\frac{\partial u}{\partial t} + \frac{\partial f(u)}{\partial x} = 0$$

on domain Ω with proper initial and boundary conditions. Ω is discretized into non-overlapping CVs $\{V_i\}$. Integrating in V_i

$$\frac{\partial \overline{u}_i}{\partial t}\Delta x_i + \int_{i-1/2}^{i+1/2} \frac{\partial f}{\partial x} dx = \frac{\partial \overline{u}_i}{\partial t}\Delta x_i + (f_{i+1/2} - f_{i-1/2}) = 0$$

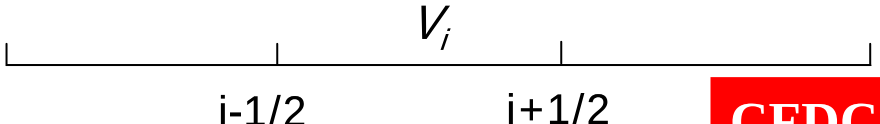

Godunov FV Method (cont.)

- Assume the solution is piece-wise constant, or a degree 0 polynomial.
- However, a new problem is created. The solution is discontinuous at the interface
- In addition, the obvious solution

$$f_{i+1/2} = [f(\overline{u}_i) + f(\overline{u}_{i+1})]/2$$

  is unstable
- A "shock-tube" problem solved to obtain the flux by Godunov

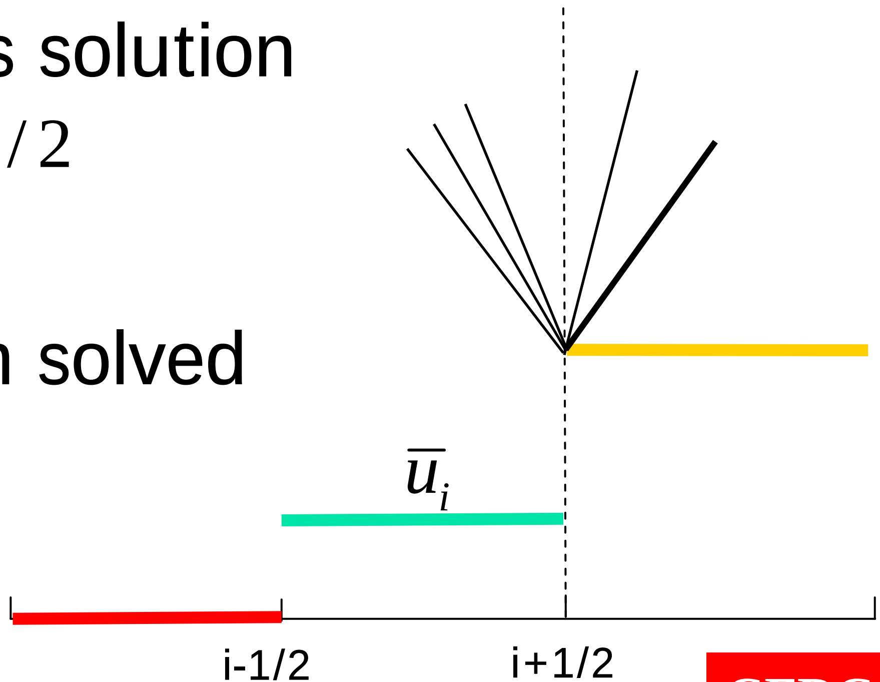

Extension to Higher-Order

- The only way to improve the solution accuracy is to increase the polynomial degree of the solution at each cell
- KEFV, DG, SV and SD methods all degenerate to the Godunov method when p = 0.
- To represent a polynomial of higher than p=0, multiple DOFs are required, e.g.,

$$U(x) = a + bx + cx^2 + \cdots$$

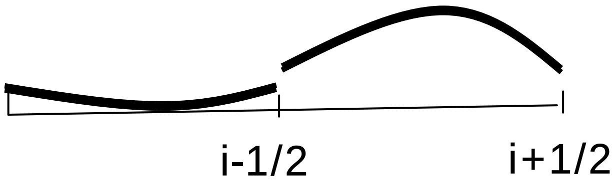

- These methods differ on how DOFs are defined and updated.

Flux Reconstruction Method

- Given the solution at SPs, build a solution polynomial in P^k
- Compute the flux at the SPs, and build an interior flux polynomial $\tilde{F}_i(x)$
- Compute Riemann fluxes at interfaces
- Find a flux polynomial $F_i(x)$ one degree higher than the solution, which minimizes

$$\left\| \tilde{F}_i(x) - F_i(x) \right\|$$

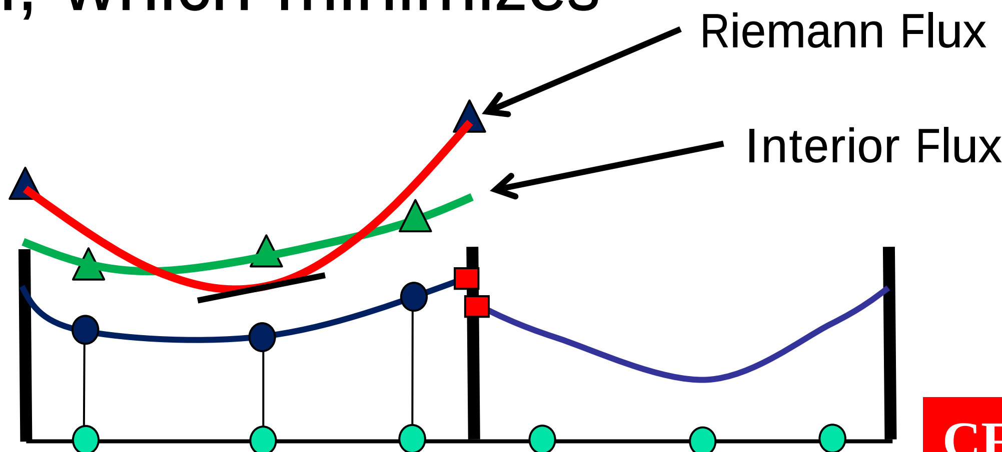

Flux Reconstruction Method (cond.)

- The use the following to update the DOFs

$$\frac{du_{i,j}}{dt} + \frac{dF_i(x_{i,j})}{dx} = 0$$

- Different conditions results in different methods. In particular, if

$$\left\| \tilde{F}_i(x) - F_i(x) \right\| \perp P^{k-1}$$

the scheme is DG

Lifting Collocation Penalty Approach

Consider

$$\frac{\partial Q}{\partial t} + \nabla \bullet \vec{F}(Q) = 0$$

The weighted residual form is

$$\int_{V_i} \left(\frac{\partial Q}{\partial t} + \nabla \bullet \vec{F}(Q) \right) W dV = \int_{V_i} \frac{\partial Q}{\partial t} W dV + \int_{\partial V_i} W \vec{F}(Q) \bullet \vec{n} dS - \int_{V_i} \nabla W \bullet \vec{F}(Q) dV$$
$$= 0.$$

Let Q^h be the discontinuous approximate solution in P^k.

The face flux integral replaced by a Riemann flux

$$\int_{V_i} \frac{\partial Q_i^h}{\partial t} W dV + \int_{\partial V_i} W \tilde{F}^n (Q_i^h, Q_{i+}^h, \vec{n}) dS - \int_{V_i} \nabla W \bullet \vec{F}(Q_i^h) dV = 0.$$

Performing integration by parts to the last term

$$\int_{V_i} \frac{\partial Q_i^h}{\partial t} W dV + \int_{V_i} W \nabla \bullet \vec{F}(Q_i^h) dV + \int_{\partial V_i} W \left[\tilde{F}^n (Q_i^h, Q_{i+}^h, \vec{n}) - F^n (Q_i^h) \right] dS = 0.$$

Lifting Collocation Penalty Approach (cont.)

Introduce the lifting operator

$$\int_{V_i} W\delta_i \, dV = \int_{\partial V_i} W\left[\tilde{F}\right] dS$$

where $\delta_i \in P^k$, $\left[\tilde{F}\right] = \left[\tilde{F}^n(Q_i^h, Q_{i+}^h, \vec{n}) - F^n(Q_i^h)\right]$. Then we have

$$\int_{V_i} \frac{\partial Q_i^h}{\partial t} W dV + \int_{V_i} W \nabla \bullet \vec{F}(Q_i^h) dV + \int_{\partial V_i} W \delta_i dV = 0,$$

which is equivalent to

$$\frac{\partial Q_i^h}{\partial t} + \nabla \bullet \vec{F}(Q_i^h) + \delta_i = 0.$$

In the new formulation, the weighting function completely disappears! Note that δ_i depends on W.

Lifting Operator – Correction Field

Obviously, the computation of δ_i is the key. From

$$\int_{V_i} W\delta_i \, dV = \int_{\partial V_i} W\left[\tilde{F}\right] dS,$$

if $\left[\tilde{F}\right], \delta_i \in P_i^k$, δ_i can be computed explicitly given W. Define a set of "flux points" along the faces, and set of solution points, where the "correction field" is computed as shown. Then

$$\delta_{i,j} = \frac{1}{|V_i|} \sum_{f \in \partial V_i} \sum_{l} \alpha_{j,f,l} [\tilde{F}]_{f,l} S_f ,$$

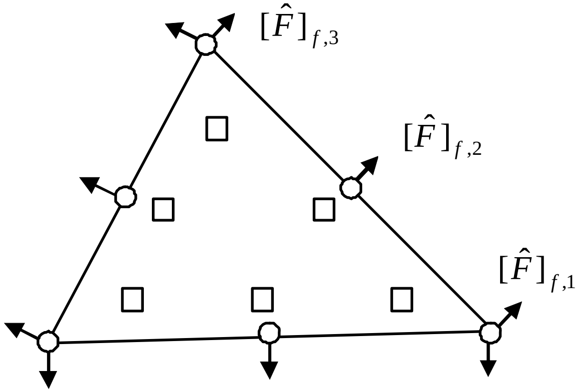

$\alpha_{j,f,l}$: lifting coefficients independent of Q

The LCP Formulation (cont.)

Finally the following equation is solved at the solution point j (collocation points)

$$\frac{\partial Q_{i,j}^{h}}{\partial t} + \nabla \bullet \vec{F}(Q_{i,j}^{h}) + \frac{1}{|V_i|} \sum_{f \in \partial V_i} \sum_{l} \alpha_{j,f,l} [\tilde{F}]_{f,l} S_f = 0.$$

The first two terms correspond to the differential equation, and the 3rd term is the "lifting penalty" term, thus the name LCP. If all the flux points coincide with the solution points, the formulation is the most efficient

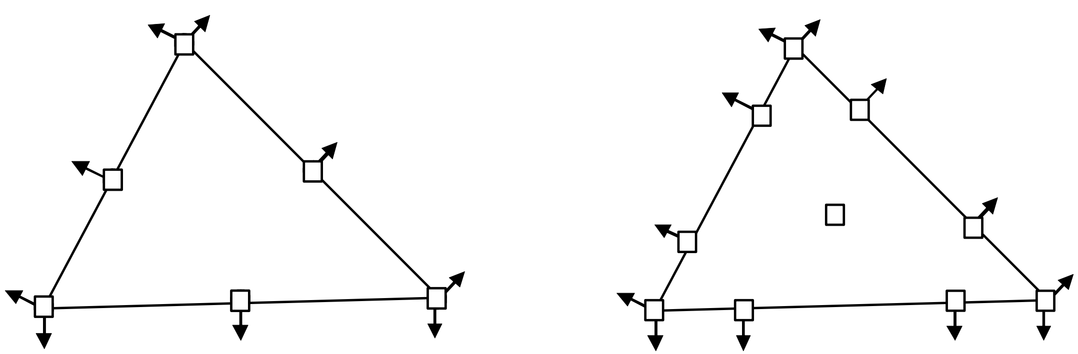

Computation of the Interior Divergence

How to compute the red term?

$$\frac{\partial Q_{i,j}^h}{\partial t} + \nabla \bullet \vec{F}(Q_{i,j}^h) + \frac{1}{|V_i|} \sum_{f \in \partial V_i} \sum_l \alpha_{j,f,l} [\tilde{F}]_{f,l} S_f = 0.$$

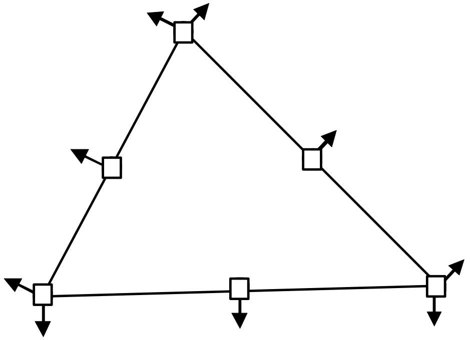

- Lagrange polynomial (LP)
  - Compute the fluxes at the solution points, and then generate Lagrange flux polynomials
  - Take the divergence at the solution points
- Chain rule (CR)

$$\nabla \bullet \vec{F}(Q_i^h) = \frac{\partial F^x(Q_i^h)}{\partial x} + \frac{\partial F^y(Q_i^h)}{\partial y} = \frac{\partial F^x}{\partial Q}\frac{\partial Q_i^h}{\partial x} + \frac{\partial F^y}{\partial Q}\frac{\partial Q_i^h}{\partial y} = \frac{\partial \vec{F}}{\partial Q} \bullet \nabla Q_i^h$$

More accurate!

Recovering the DG, SV and SD Methods

- Let $W \in P^k$, the DG method is exactly recovered, at least in the linear case. For k = 1,

$$\delta_{i,1} = \frac{1}{|V_i|}\left[(2.5[\tilde{F}]_{1,1} + 0.5[\tilde{F}]_{1,2})S_1 + (-1.5[\tilde{F}]_{2,1} - 1.5[\tilde{F}]_{2,2})S_2 + (0.5[\tilde{F}]_{3,1} + 2.5[\tilde{F}]_{3,2})S_3\right]$$

- For the SV method, select piece-wise constant W

$$\delta_{i,1} = \frac{1}{|V_i|}\left[(2[\tilde{F}]_{1,1} + 0.2[\tilde{F}]_{1,2})S_1 + (-0.7[\tilde{F}]_{2,1} - 0.7[\tilde{F}]_{2,2})S_2 + (0.2[\tilde{F}]_{3,1} + 2[\tilde{F}]_{3,2})S_3\right]$$

- For the SD method, more involved but doable for equilateral triangle

$$\delta_{i,1} = \frac{1}{|V_i|}\left[2[\tilde{F}]_{1,1}S_1 + (-0.5[\tilde{F}]_{2,1} - 0.5[\tilde{F}]_{2,2})S_2 + 2[\tilde{F}]_{3,2}S_3\right]$$

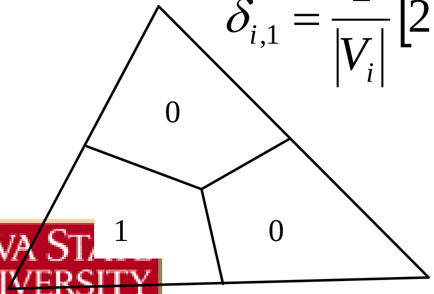

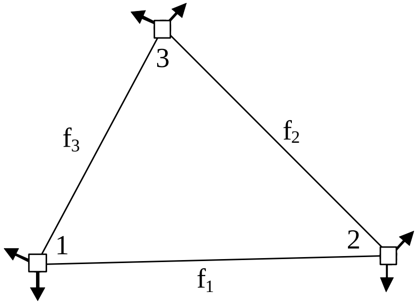

LCP Algorithm

- Compute the cell interior divergence using either the LP or CR approaches (no-coupling);
- Compute the Riemann fluxes at the flux points, and also compute the normal component of the interior flux;
- Scatter the corrections to the elements

$$\frac{\partial Q_{i,j}^h}{\partial t} + \nabla \bullet \vec{F}(Q_{i,j}^h) + \frac{1}{|V_i|}\sum_{f \in \partial V_i}\sum_{l} \alpha_{j,f,l}[\tilde{F}]_{f,l} S_f = 0.$$

Advantages:

- No reconstruction cost
- No mass matrix

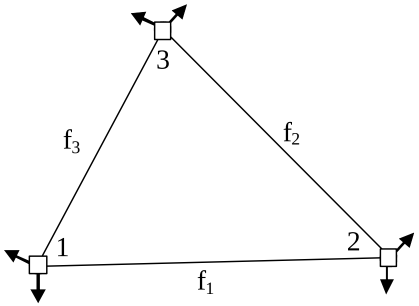

Mixed Grids

- In order to minimize data reconstruction and communication, solution points coincide with flux points
- For quadrilateral elements, the corrections are one-dimensional!
- Mass matrix is I for all cell-types

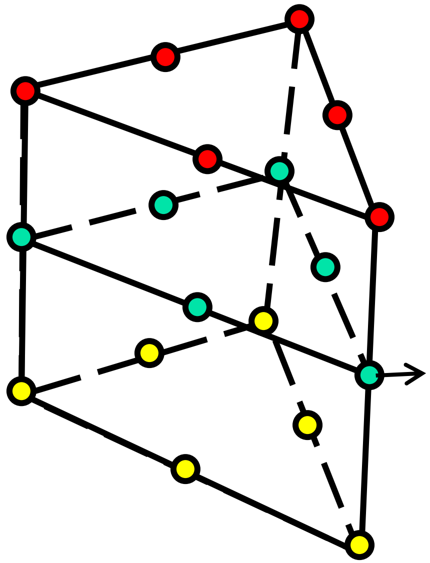

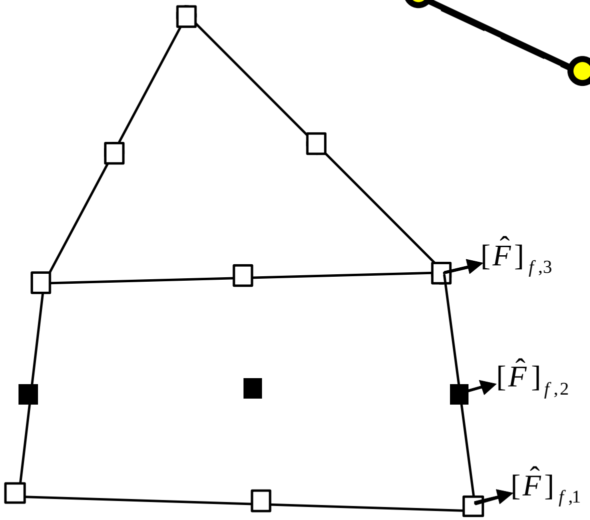

Curved Boundaries

- Transform the governing equations from the (curved) physical domain to the (straight) computational domain;
- The LCP formulation is then applied to the transformed equations in the standard element
- Straightforward!

$$\frac{\partial \tilde{Q}}{\partial t} + \frac{\partial F^{\xi}}{\partial \xi} + \frac{\partial F^{\eta}}{\partial \eta} = 0$$

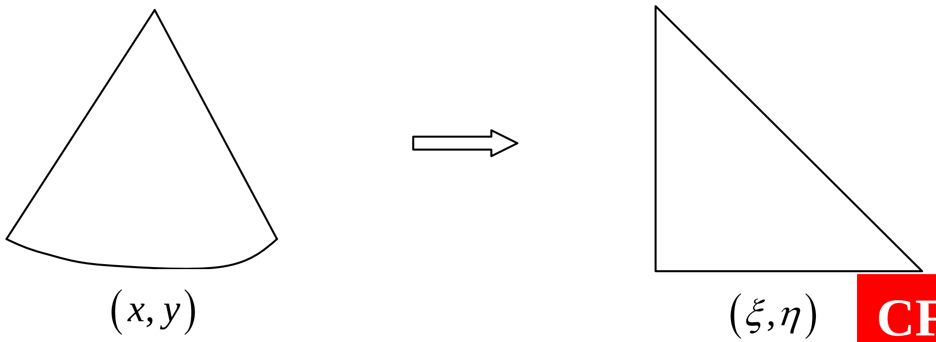

Test Cases

- Accuracy studies for scalar conservation laws;
- Accuracy study for the Euler equations
- Flow over a cylinder
- Flow over a NACA0012 airfoil
- Flow over a sphere

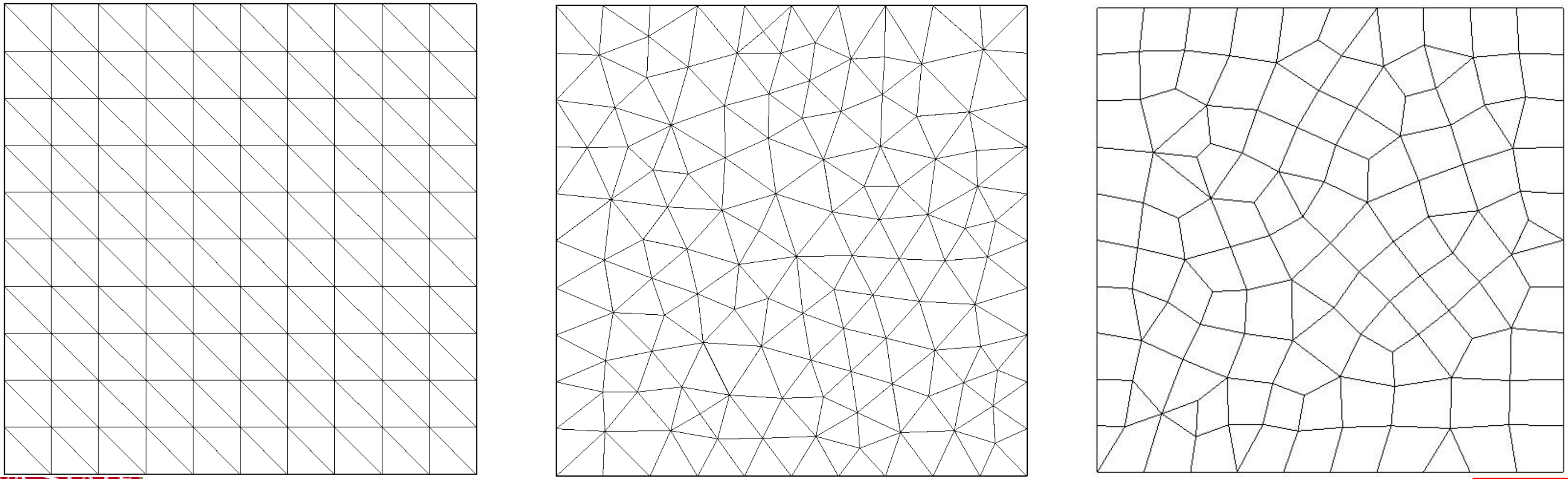

$$u_t + u_x + u_y = 0,\ with\ u_0(x, y) = \sin \pi (x + y),\ at\ t = 1$$

- LCP-DG

Polynomial degree k	*Grid size*	Regular Mesh		Irregular Mesh	
		L2 error	Order	L2 error	Order
1	10x10x2	2.44e-2	-	4.45e-2	-
	20x20x2	5.89e-3	2.05	1.05e-2	2.08
	40x40x2	1.46e-3	2.01	2.57e-3	2.03
	80x80x2	3.64e-4	2.00	6.41e-4	2.00
2	10x10x2	1.88e-3	-	3.99e-3	-
	20x20x2	2.38e-4	2.98	5.14e-4	2.96
	40x40x2	2.98e-5	3.00	6.47e-5	2.99
	80x80x2	3.73e-6	3.00	8.10e-6	3.00
3	10x10x2	7.55e-5	-	2.59e-4	-
	20x20x2	4.94e-6	3.93	1.59e-5	4.03
	40x40x2	3.08e-7	4.00	9.91e-7	4.00
	80x80x2	1.93e-8	4.00	6.19e-8	4.00
5	10x10x2	7.53e-8	-	5.87e-7	-
	20x20x2	1.18e-9	6.00	9.22e-9	5.99
	40x40x2	1.85e-11	6.00	1.43e-10	6.01

$$u_t + u_x + u_y = 0, \textit{ with } u_0(x, y) = \sin \pi (x + y), \textit{ at } t = 1$$

- LCP-SV

Polynomial degree k	*Grid size*	Regular Mesh		Irregular Mesh	
		L_2 *error*	Order	L_2 *error*	Order
1	10x10x2	5.94e-2	-	1.01e-1	-
	20x20x2	1.45e-2	2.03	2.62e-2	1.95
	40x40x2	3.72e-3	1.96	6.55e-3	2.00
	80x80x2	9.23e-4	2.01	1.63e-3	2.01
2	10x10x2	2.84e-3	-	7.47e-3	-
	20x20x2	3.71e-4	2.94	9.09e-4	3.04
	40x40x2	4.73e-5	2.97	1.13e-4	3.01
	80x80x2	5.97e-6	2.99	1.42e-5	2.99
3	10x10x2	1.04e-4	-	4.37e-4	-
	20x20x2	6.53e-6	3.99	2.58e-5	4.08
	40x40x2	4.11e-7	3.99	1.56e-6	4.05
	80x80x2	2.57e-8	4.00	9.61e-8	4.02

$$u_t + uu_x + uu_y = 0, \; with \; u_0(x,y) = 0.25 + 0.5\sin\pi(x+y), \; at \; t = .1$$

❖ LCP-DG on irregular mesh

Polynomial degree k	*Grid size*	Irregular Mesh (LP)		Irregular Mesh (CR)	
		L_2 *error*	Order	L_2 *error*	Order
1	10x10x2	2.65e-2	-	1.84e-2	-
	20x20x2	9.96e-3	1.41	5.06e-3	1.86
	40x40x2	3.75e-3	1.41	1.35e-3	1.91
	80x80x2	1.38e-3	1.44	3.50e-4	1.95
2	10x10x2	6.40e-3	-	2.75e-3	-
	20x20x2	1.37e-3	2.20	4.04e-4	2.77
	40x40x2	2.81e-4	2.29	5.50e-5	2.88
	80x80x2	5.43e-5	2.37	7.27e-6	2.92
3	10x10x2	9.59e-4	-	3.68e-4	-
	20x20x2	1.05e-4	3.19	2.58e-5	3.83
	40x40x2	9.86e-6	3.41	1.82e-6	3.83
	80x80x2	8.48e-7	3.54	1.27e-7	3.84
5	10x10x2	3.46e-5		1.07e-5	-
	20x20x2	1.15e-6	4.91	2.61e-7	5.35
	40x40x2	3.15e-8	5.19	4.45e-9	5.87
	80x80x2	7.08e-10	5.48	8.27e-11	5.75

Accuracy Study with the Euler Equations

- Vortex propagation problem

Polynomial degree k	*Grid size*	Irregular Triangular Mesh - Test 1 (LP)		Irregular Triangular Mesh - Test 2 (CR)		Mixed Mesh (CR)	
		L_2 *error*	Order	L_2 *error*	Order	L_2 *error*	Order
1	10x10x2	2.01e-2	-	1.39e-2	-	1.58e-2	-
	20x20x2	6.67e-3	1.59	4.41e-3	1.66	5.32e-3	1.57
	40x40x2	1.73e-3	1.95	1.08e-3	2.03	1.50e-3	1.83
	80x80x2	4.84e-4	1.84	2.54e-4	2.09	3.54e-4	2.08
2	10x10x2	7.14e-3	-	4.41e-3	-	2.95e-3	-
	20x20x2	1.07e-3	2.74	5.19e-4	3.09	5.62e-4	2.39
	40x40x2	1.60e-4	2.74	5.84e-5	3.15	7.42e-5	2.92
	80x80x2	2.29e-5	2.80	6.94e-6	3.07	8.63e-6	3.10
3	10x10x2	1.79e-3	-	6.70e-4	-	5.79e-4	-
	20x20x2	1.40e-4	3.68	4.79e-5	3.81	5.05e-5	3.52
	40x40x2	9.75e-6	3.84	2.96e-6	4.02	3.51e-6	3.85
	80x80x2	6.96e-7	3.81	1.71e-7	4.11	1.89e-7	4.22

Inviscid Flow over a Cylinder - Triangles

- Mach = 0.3, LCP-DG, 4th Order

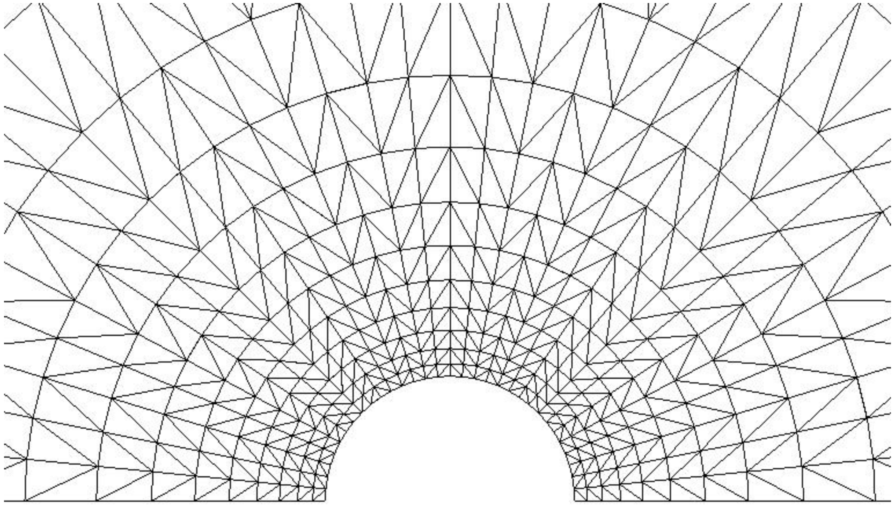

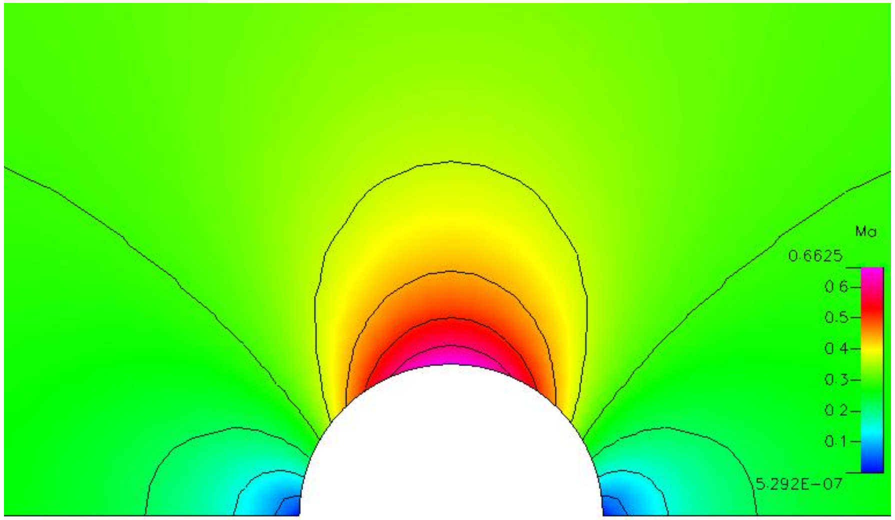

Inviscid Flow over a Cylinder – Hybrid 1

- Mach = 0.3, LCP-FR-DG, 4th Order

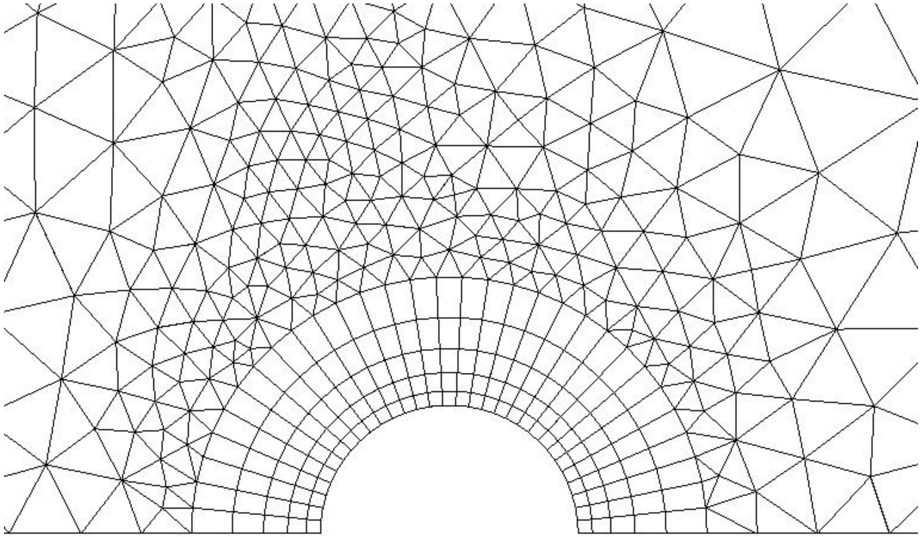

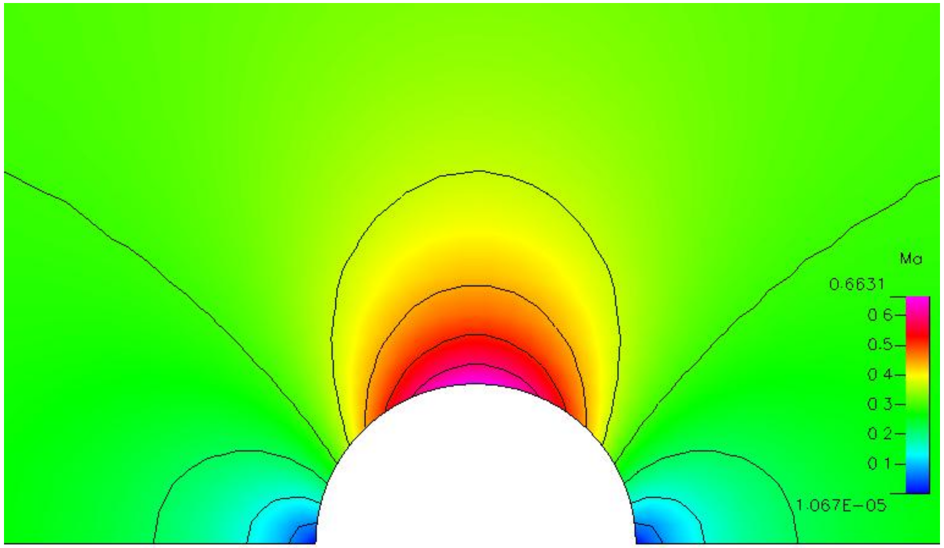

Inviscid Flow over a Cylinder – Hybrid 2

- Mach = 0.3, LCP-FR-DG, 4th Order

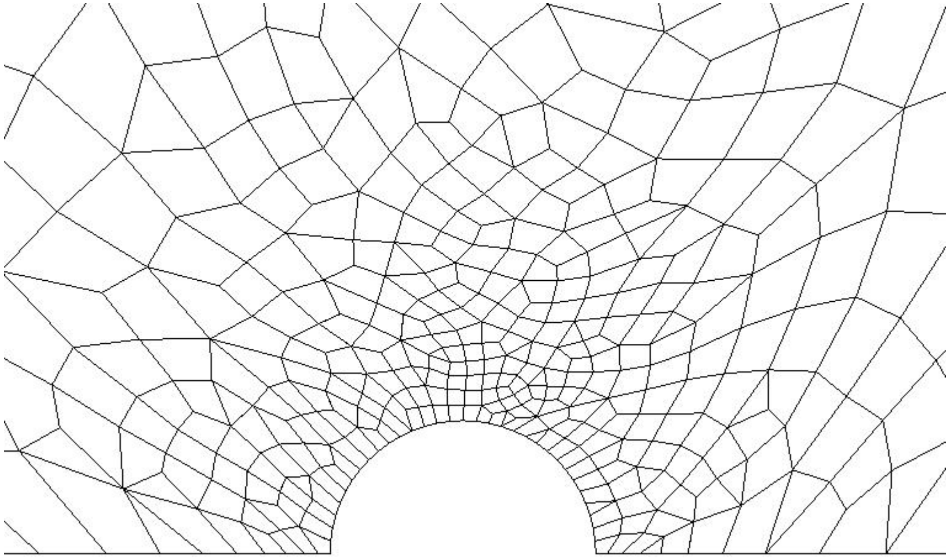

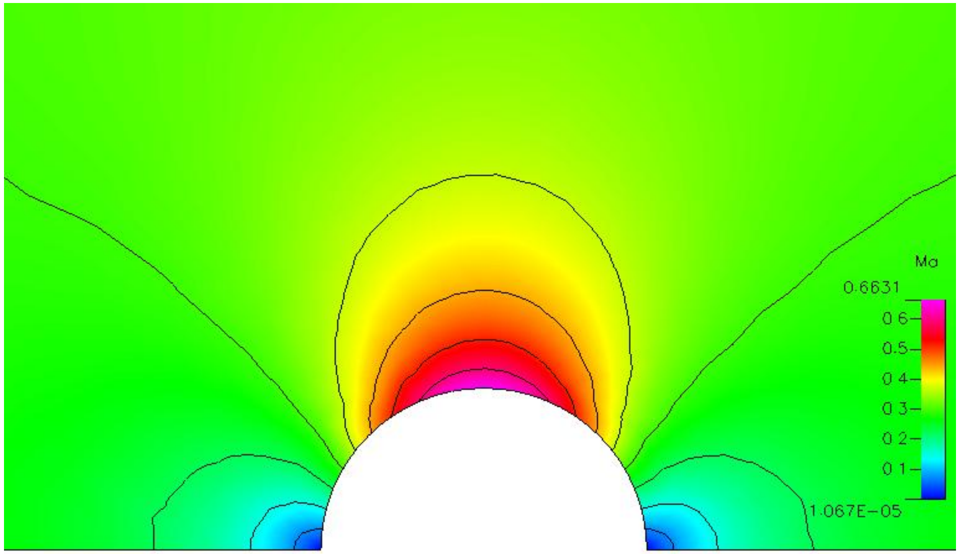

Flow over NACA0012 Airfoil – Hybrid Mesh

- Mach = 0.3, α = 5 degrees, LCP-FR-DG, 2nd-4th Order

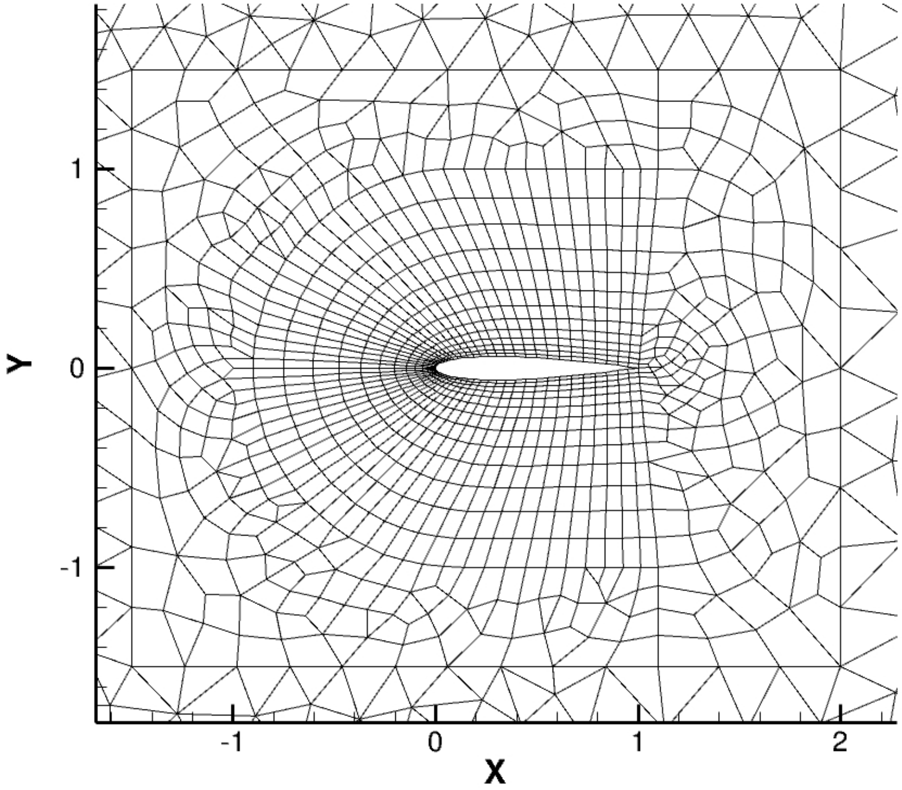

Flow over NACA0012 Airfoil – Hybrid Mesh

- Mach = 0.3, α = 5 degrees, 2nd Order

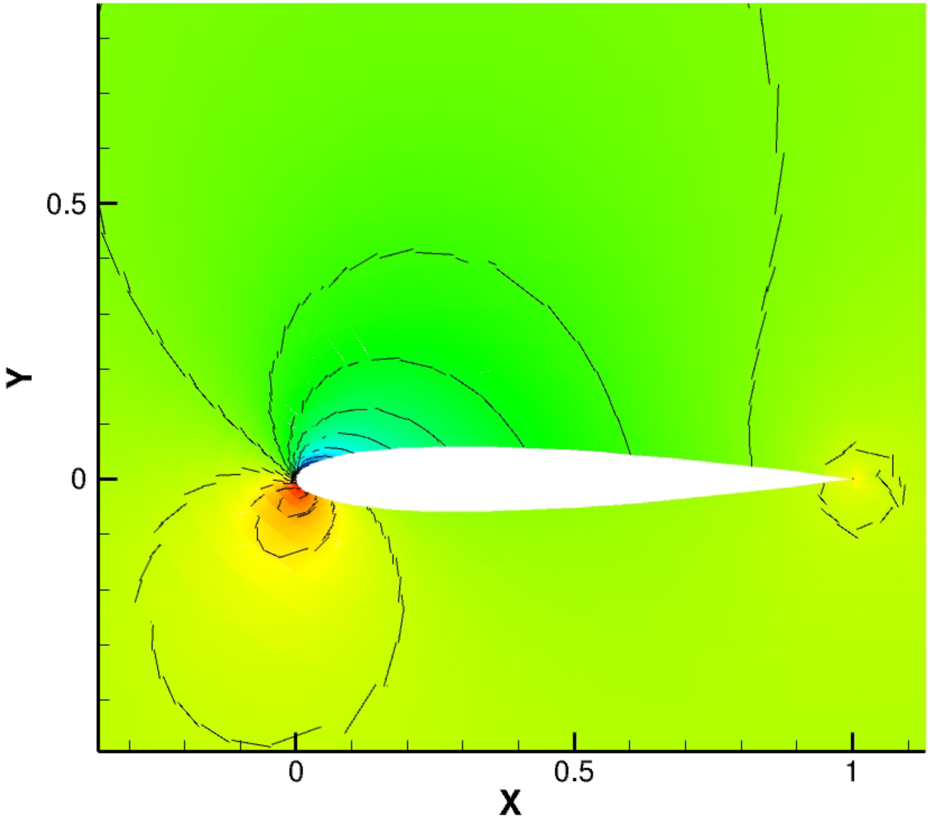

Pressure

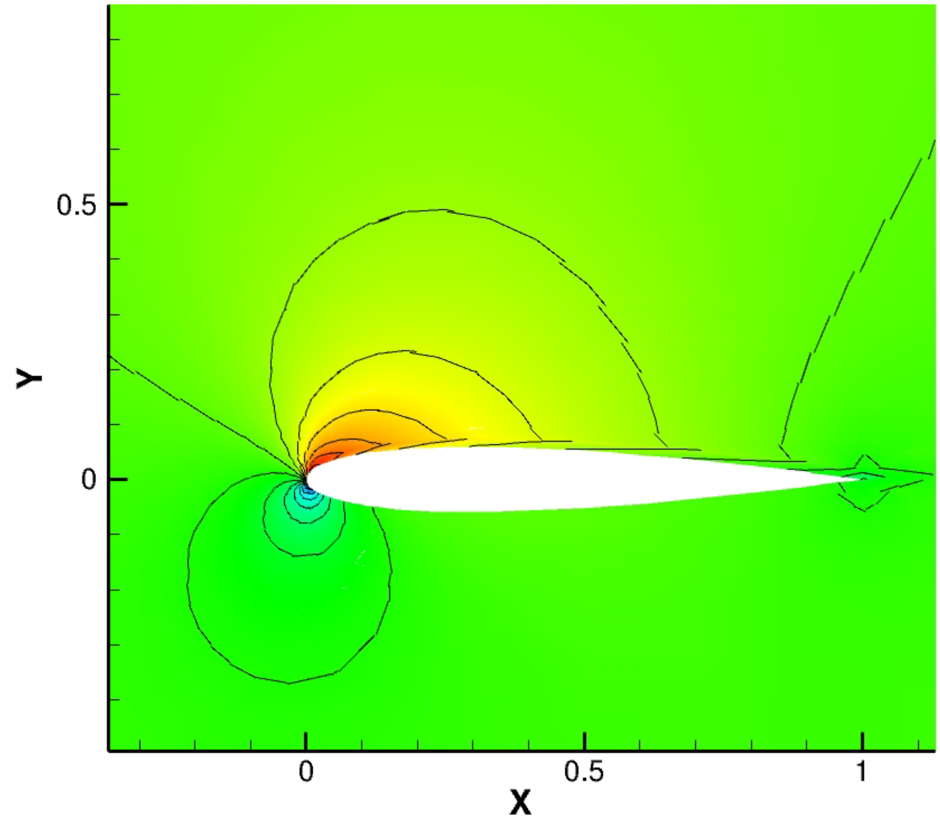

Mach

Flow over NACA0012 Airfoil – Hybrid Mesh

- Mach = 0.3, α = 5 degrees, 3[rd] Order

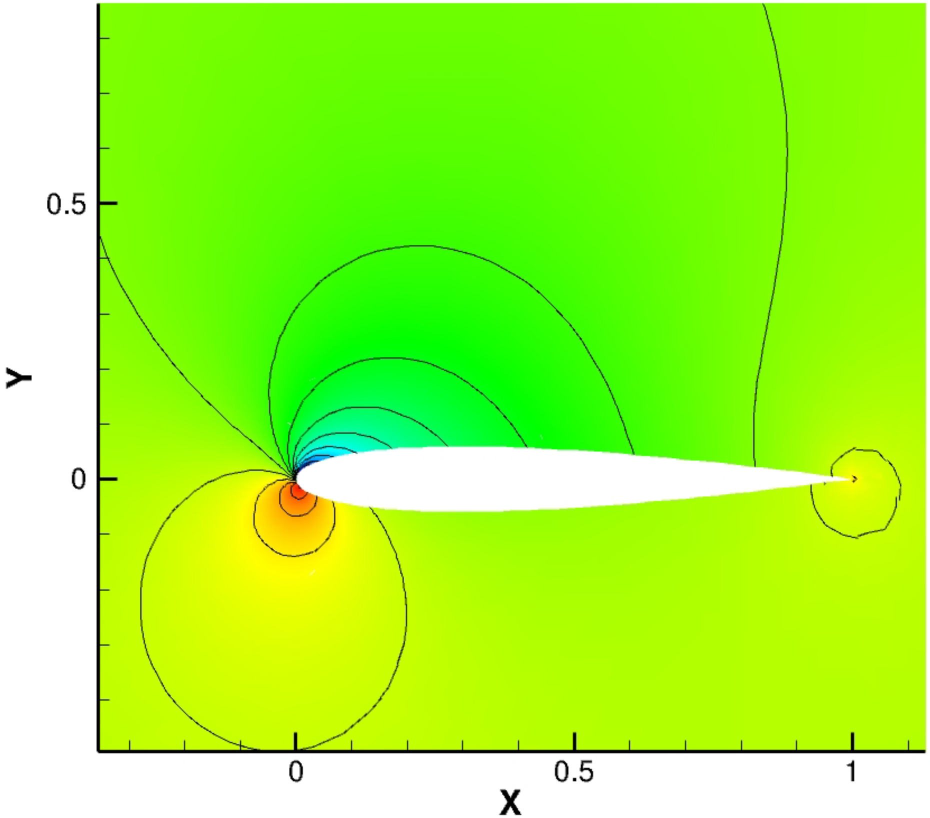

Pressure

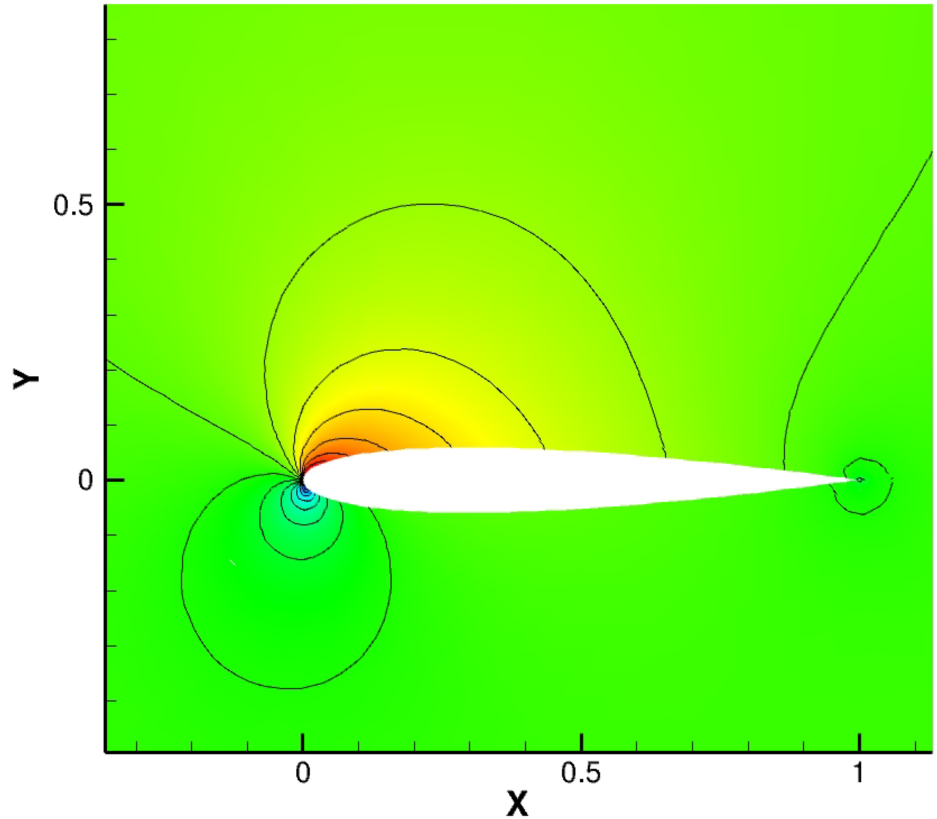

Mach

Flow over NACA0012 Airfoil – Hybrid Mesh

- Mach = 0.3, α = 5 degrees, 4th Order

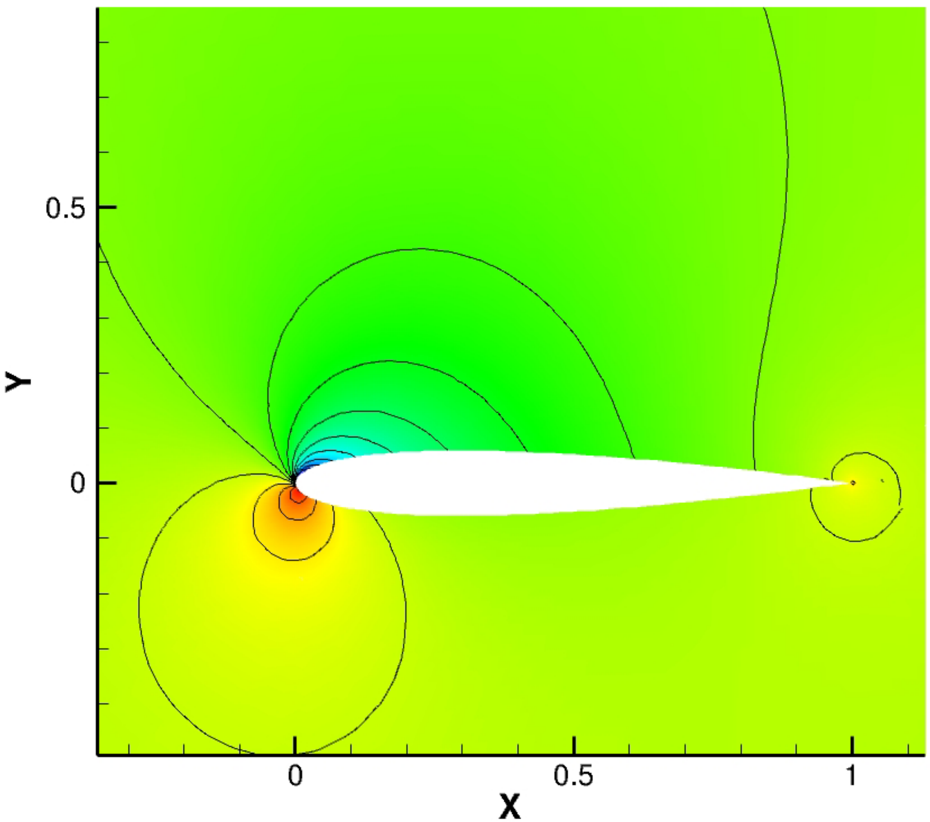

Pressure

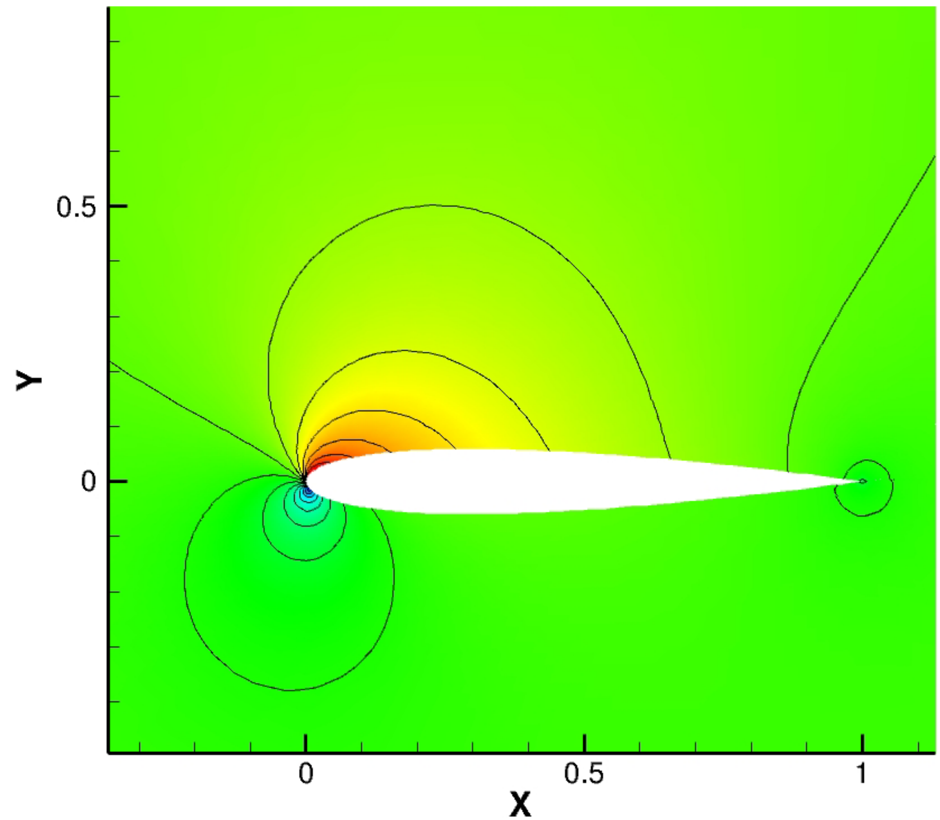

Mach

Flow over NACA0012 Airfoil – Hybrid Mesh

- Wall entropy error

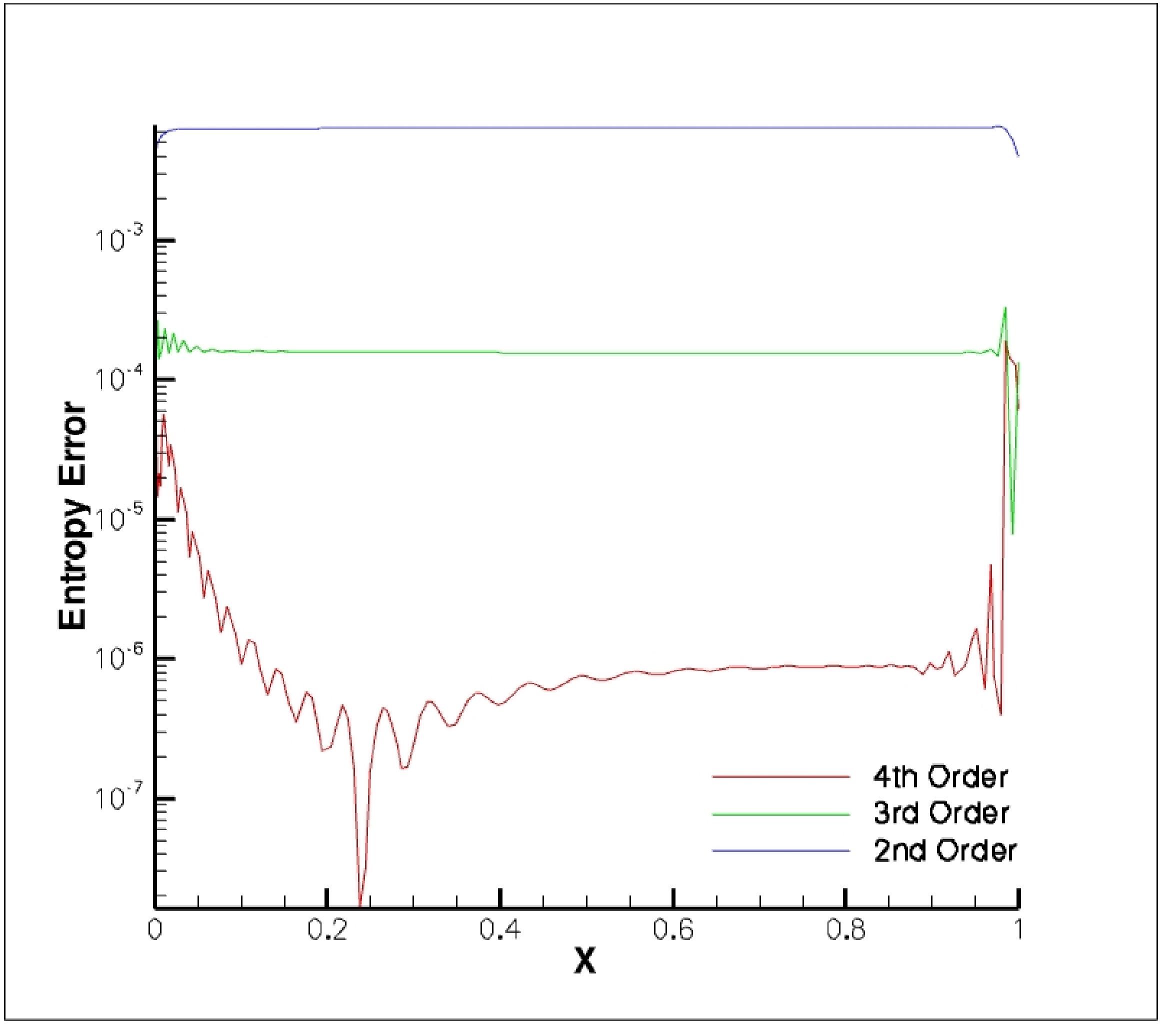

Inviscid Flow Over 1/4 Sphere

- Freestream: $M_\infty = 0.3$

- Numerical Methods:
  - LCP (2nd-4th order)
  - 3 stage Runge-Kutta / LU-SGS
  - Curved wall treatment (quadratic polynomials)

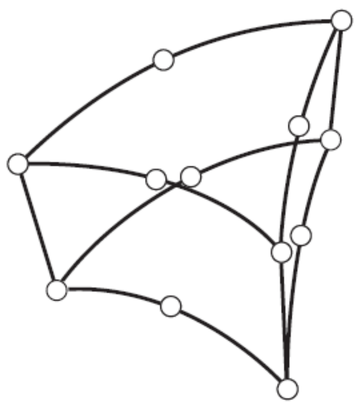

- Prism mesh:

Points 49×31=1519, Cells 80×30=2400

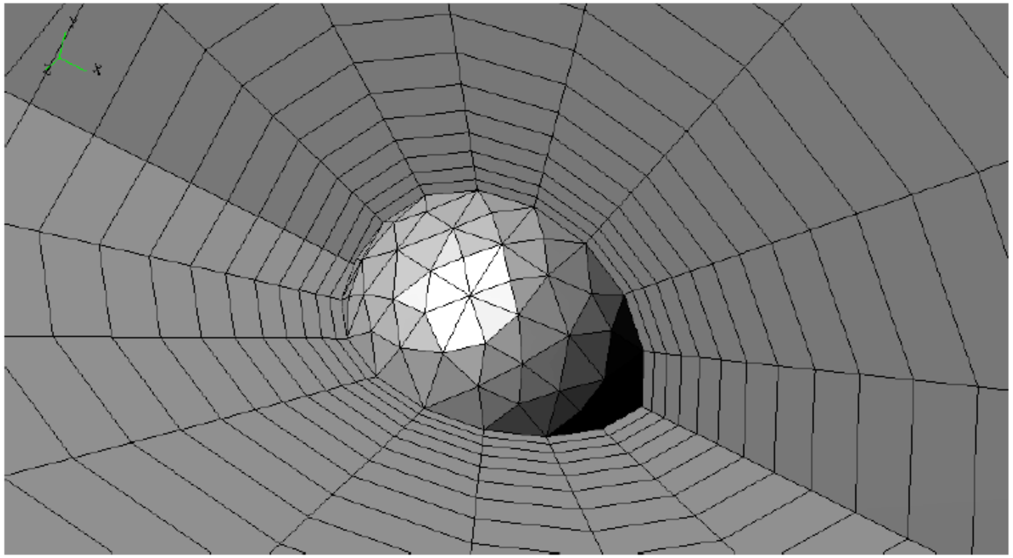

Prism Mesh for 1/4 Sphere

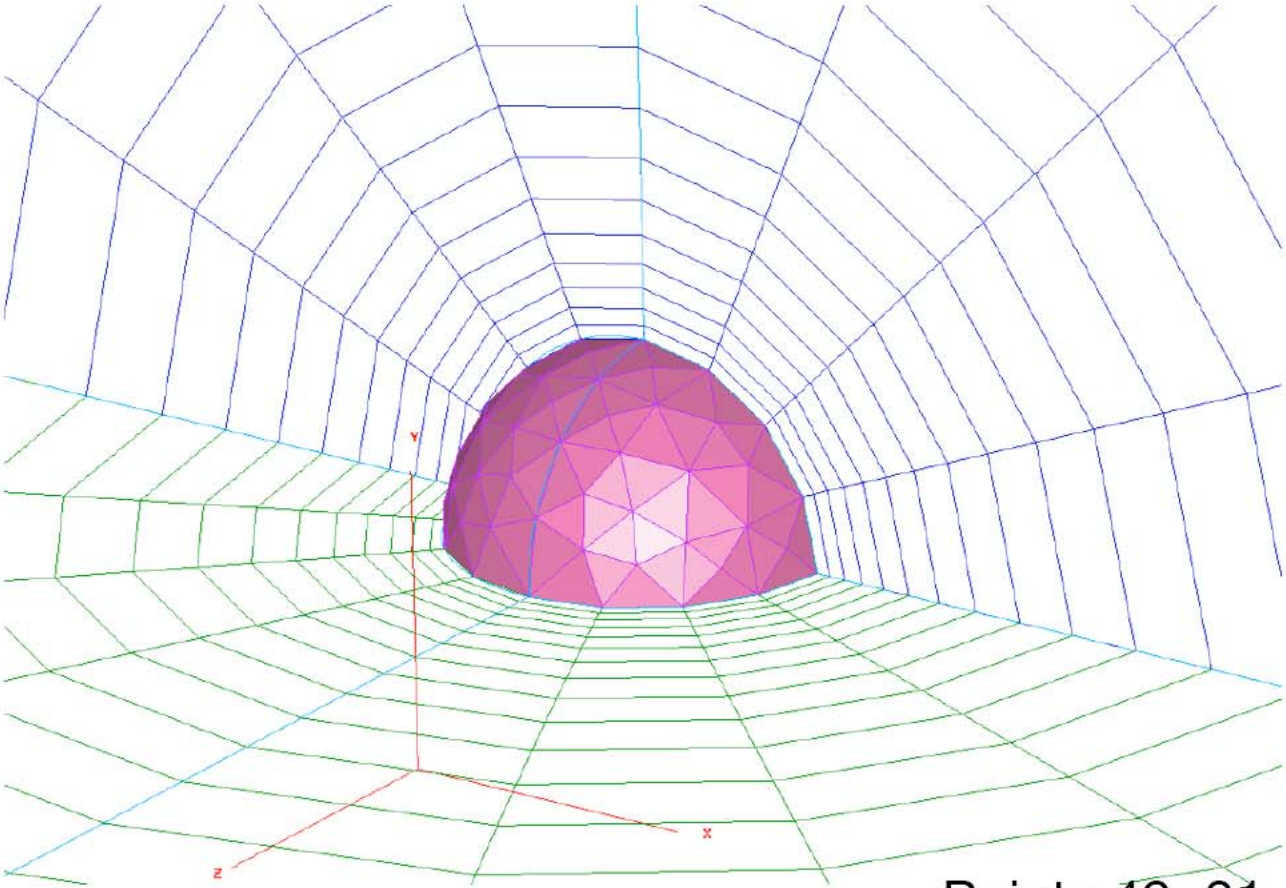

Points 49×31=1519

Cells 80×30=2400

Tetra-Prism Mixed Mesh for 1/4 Sphere

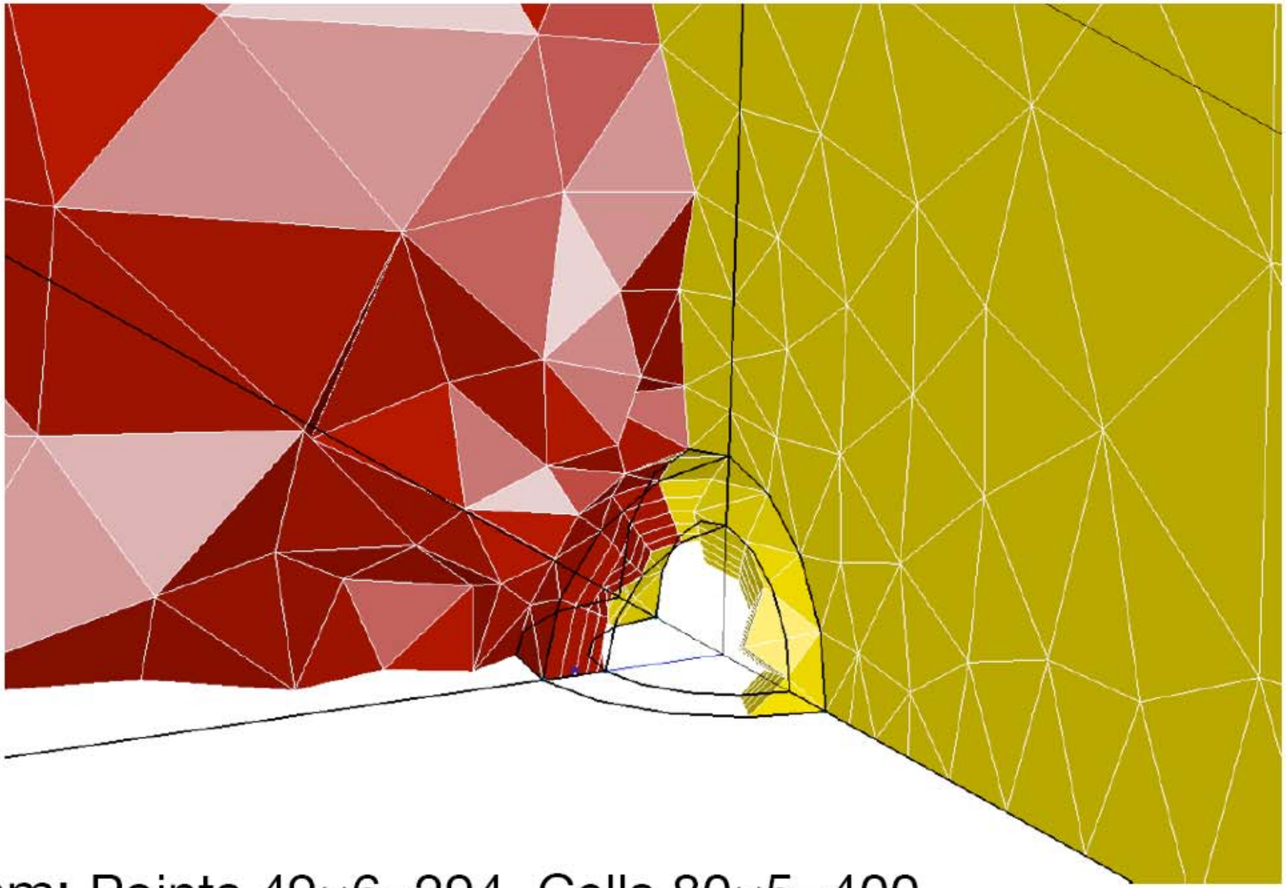

- Prism: Points 49×6=294, Cells 80×5=400
- Tetra: Points 512, Cells 2026

Density Contours (LCP-DG, Prism)

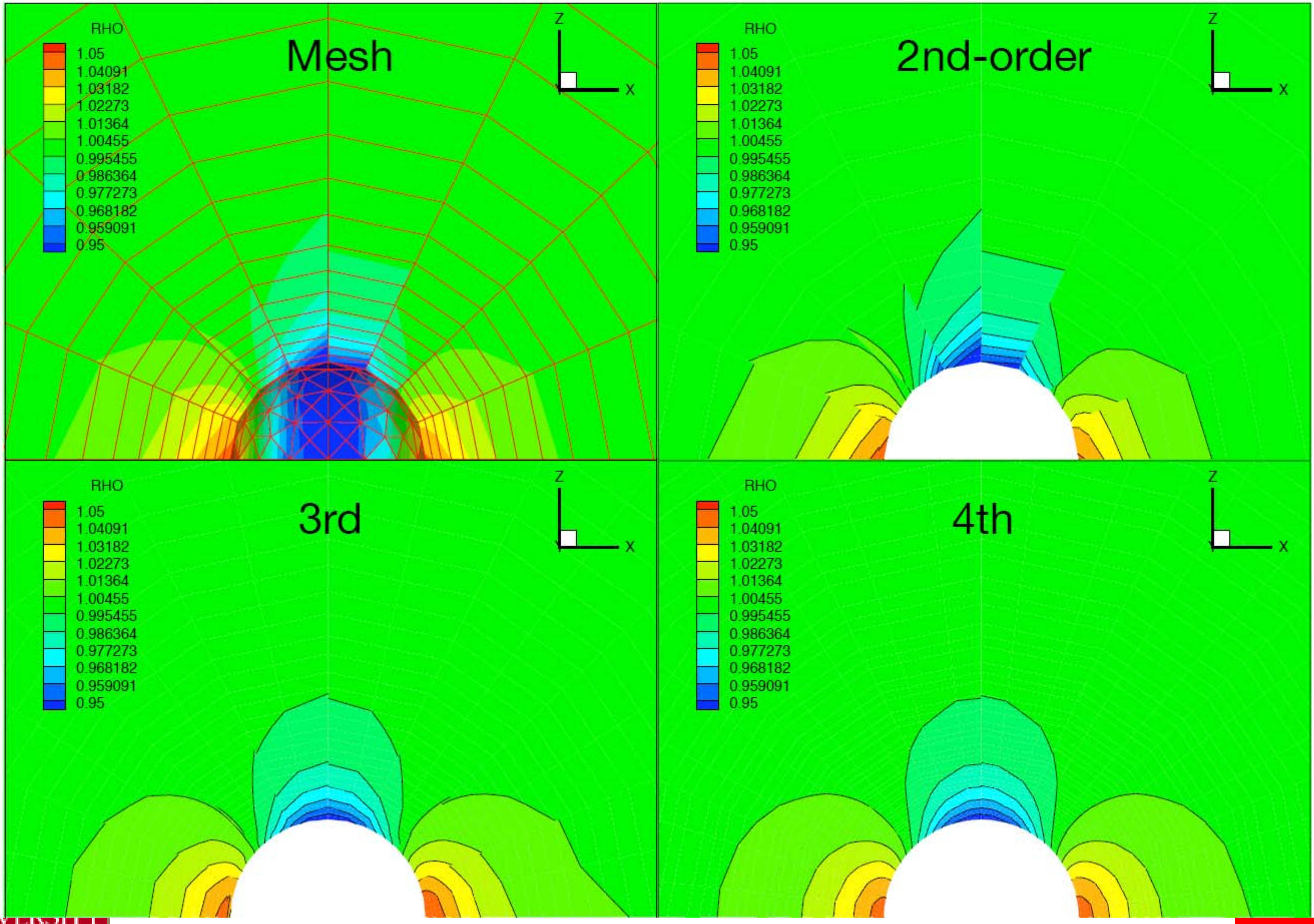

Density Contours (LCP-DG, Tetra & Prism)

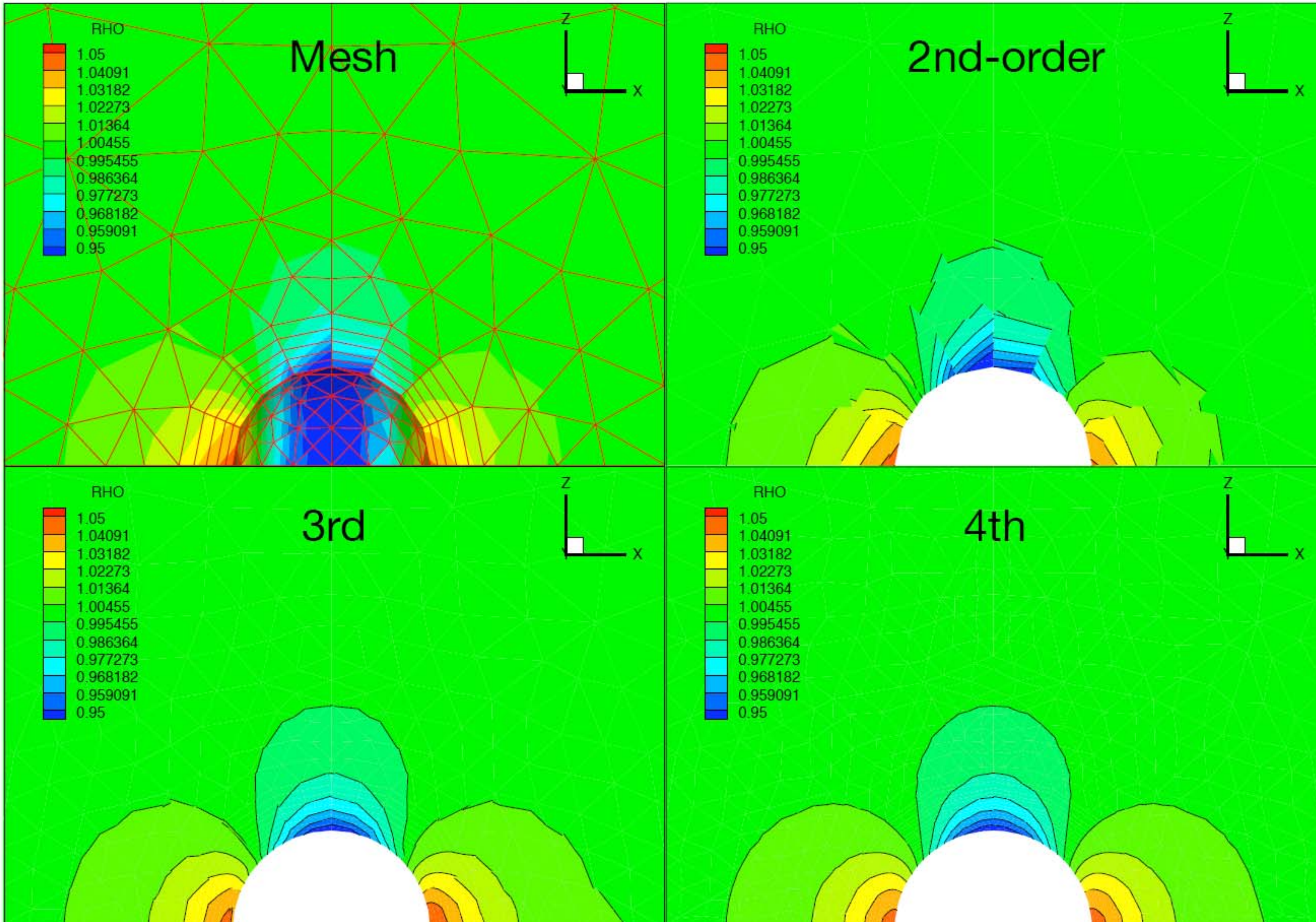

Conclusions and Future Work

- A lifting collocation penalty formulation is successfully developed for simplex cells, which is a generalization of the flux reconstruction method;
- The formulation unifies the DG, SV and in a special case the SD method into a single family;
- Weighting functions disappear from the formulation. Their effects are implicitly embedded in the lifting coefficients;

Conclusions and Future Work (cont.)

- The extension to mixed grids and curved boundary straightforward because no surface or volume integrals involved
- Accuracy studies and benchmark test cases demonstrated the performance of the method
- The extension to the Navier-Stokes equations are under way and will be reported in the future.

Acknowledgements

- We are grateful to AFOSR and Iowa State University for supporting the research;
- Questions?